

---

1     Aerosol Composition and Sources during the Chinese Spring  
2     Festival: Fireworks, Secondary Aerosol, and Holiday Effects

3  
4                   Qi Jiang<sup>1,3</sup>, Yele Sun<sup>1,2\*</sup>, Zifa Wang<sup>1</sup>, Yan Yin<sup>2,3</sup>

5  
6     <sup>1</sup>State Key Laboratory of Atmospheric Boundary Layer Physics and Atmospheric  
7     Chemistry, Institute of Atmospheric Physics, Chinese Academy of Sciences, Beijing  
8                   100029, China

9     <sup>2</sup>Collaborative Innovation Center on Forecast and Evaluation of Meteorological  
10    Disasters, Nanjing University of Information Science & Technology, Nanjing, 210044,  
11                   China

12    <sup>3</sup>Key Laboratory for Aerosol-Cloud-Precipitation of China Meteorological Administra  
13    tion, Nanjing University of Information Science & Technology, Nanjing 210044, China

14  
15  
16  
17                   Correspondence to: sunyele@mail.iap.ac.cn

---

18 **Abstract**

19 Aerosol particles were characterized by an Aerodyne Aerosol Chemical Speciation  
20 Monitor (ACSM) along with various collocated instruments in Beijing, China to  
21 investigate the roles of fireworks (FW) and secondary aerosol in particulate pollution  
22 during the Chinese Spring Festival of 2013. Three fireworks events exerting significant  
23 and short-term impacts on fine particles ( $PM_{2.5}$ ) were observed on the days of Lunar  
24 New Year, Lunar Fifth Day, and Lantern Festival. The FW showed large impacts on  
25 non-refractory potassium, chloride, sulfate, and organics in submicron aerosol ( $PM_1$ ),  
26 of which the FW organics appeared to be emitted mainly in secondary with its mass  
27 spectrum resembling to that of secondary organic aerosol (SOA). Pollution events (PEs)  
28 and clean periods (CPs) alternated routinely throughout the study. Secondary  
29 particulate matter ( $SPM = SOA + \text{sulfate} + \text{nitrate} + \text{ammonium}$ ) dominated the total  
30  $PM_1$  mass on average accounting for 63-82% during nine PEs in this study. The  
31 elevated contributions of secondary species during PEs resulted in a higher mass  
32 extinction efficiency of  $PM_1$  ( $6.4 \text{ m}^2 \text{ g}^{-1}$ ) than that during CPs ( $4.4 \text{ m}^2 \text{ g}^{-1}$ ). The Chinese  
33 Spring Festival also provides a unique opportunity to study the impacts of reduced  
34 anthropogenic emissions on aerosol chemistry in the city. The primary species showed  
35 ubiquitous reductions during the holiday period with the largest reduction for cooking  
36 OA (69%), nitrogen monoxide (54%), and coal combustion OA (28%). The secondary  
37 sulfate, however, remained minor change, and the SOA and the total  $PM_{2.5}$  even slightly  
38 increased. Our results have significant implications that controlling local primary  
39 source emissions during PEs, e.g., cooking and traffic activities, might have limited  
40 effects on improving air quality in megacity Beijing due to the dominance of SPM from  
41 regional transport in aerosol particle composition.

---

## 42 1 Introduction

43 Air pollution caused by fine particles (PM<sub>2.5</sub>) is of great concern in densely  
44 populated megacities because of its adverse effects on human health and regional air  
45 quality (Molina and Molina, 2004; Chan and Yao, 2008). The health risk of air  
46 pollution is greater than expected leading to around 7 million people's death in 2012  
47 according to the latest report by World Health Organization  
48 (<http://www.who.int/mediacentre/news/releases/2014/air-pollution/en/>). The Beijing  
49 metropolitan area is one of the most populous megacities in the world with the  
50 population reaching 20.69 million by the end of 2012 (Beijing Municipal Bureau of  
51 Statistics). According to Beijing Municipal Environmental Protection Bureau, the  
52 annual average concentration of PM<sub>2.5</sub> was 89.5 µg m<sup>-3</sup> in 2013, which is about 2.5  
53 times the National Ambient Air Quality Standards of China (35 µg m<sup>-3</sup> for annual  
54 average). This suggests severe fine particle pollution in Beijing. Extensive studies  
55 have been made recently to investigate the chemical composition and sources of PM<sub>2.5</sub>.  
56 The results showed that secondary inorganic aerosol (SIA = sulfate + nitrate +  
57 ammonium), coal combustion, traffic emissions (gasoline and diesel), biomass  
58 burning, cooking emissions and dust are the major sources of PM<sub>2.5</sub> (Zheng et al.,  
59 2005; Song et al., 2006; Zhang et al., 2013). However, the source contributions varied  
60 significantly among different seasons, therefore improving air quality in Beijing  
61 remains a great challenge due to the very complex sources and dynamic evolution  
62 processes of aerosol particles.

63 Fine particles from various sources can be either primary from direct emissions,  
64 e.g., fossil fuel combustion and biomass burning, or secondary from atmospheric  
65 oxidation of gas-phase species. The fireworks (FW) is one of the most important

---

66 primary sources that can exert significant and short-time impacts on air quality. The  
67 fireworks burning emits a large amount of gaseous pollutants, e.g., sulfur dioxide  
68 (SO<sub>2</sub>) and nitrogen oxide (NO<sub>x</sub>) (Vecchi et al., 2008;Huang et al., 2012), and also fine  
69 particles comprising organic/elemental carbon, sulfate, potassium, chloride and  
70 various metals, e.g., copper (Cu), barium (Ba), strontium (Sr) and magnesium (Mg)  
71 (Moreno et al., 2007;Wang et al., 2007;Li et al., 2013). The enhanced short-term air  
72 pollution by fireworks can substantially increase health risk levels (Godri et al.,  
73 2010;Yang et al., 2014) and reduce visibility for hours (Vecchi et al., 2008). Previous  
74 studies on chemical characterization of fireworks in China were mostly based on filter  
75 measurements with a time resolution of 12 h or 24 h (Wang et al., 2007;Zhang et al.,  
76 2010;Feng et al., 2012;Huang et al., 2012;Cheng et al., 2014;Zhao et al., 2014).  
77 Considering that the fireworks events usually last less than 12 hours, the filter analysis  
78 may introduce large uncertainties in accurate quantification of chemical composition  
79 of FW particles due to either the interferences of non-FW (NFW) background  
80 aerosols or the difficulties to account for meteorological variations. Drewnick et al.  
81 (2006) first conducted real-time size-resolved chemical composition measurements  
82 during the New Year's period in Mainz, Germany using an Aerodyne Time-of-Flight  
83 Aerosol Mass Spectrometer (ToF-AMS). To our knowledge, there are no such  
84 real-time measurements of chemical composition of aerosol particles during fireworks  
85 events in China yet, which limits our understanding on the rapid formation and  
86 evolution of fireworks events, and also their impacts on particulate matter (PM)  
87 pollution.

88       Secondary aerosol is of more concern compared to primary aerosol because it is  
89 formed over regional scales and exerts impacts on air quality over wider areas (Matsui

---

90 et al., 2009;DeCarlo et al., 2010). Therefore, extensive studies have been conducted in  
91 recent years to characterize the sources and formation mechanisms of secondary  
92 aerosol (Yao et al., 2002;Duan et al., 2006;Sun et al., 2006;Wang et al., 2006;Guo et  
93 al., 2010;Yang et al., 2011;Sun et al., 2013b;Zhang et al., 2013;Zhao et al., 2013).  
94 SIA was observed to contribute a large fraction of PM<sub>2.5</sub> and played an enhanced role  
95 during haze episodes due to the faster heterogeneous reactions associated with higher  
96 humidity (Liu et al., 2013;Sun et al., 2013a;Zhao et al., 2013;Sun et al., 2014;Wang et  
97 al., 2014). While SIA was relatively well characterized, secondary organic aerosol  
98 (SOA) is not well understood (Huang et al., 2014). The recent deployments of  
99 Aerodyne Aerosol Mass Spectrometers (AMS) greatly improved our understanding  
100 on sources and evolution processes of organic aerosol (OA) in China, and also the  
101 different roles of primary organic aerosol (POA) and SOA in PM pollution (Huang et  
102 al., 2010;Sun et al., 2010;He et al., 2011;Sun et al., 2012;Sun et al., 2013b;Zhang et  
103 al., 2014). While SOA is more significant in summer (Huang et al., 2010;Sun et al.,  
104 2010;Sun et al., 2012), POA generally plays a more important role during wintertime  
105 (Sun et al., 2013b). Recently, the role of SOA in fine particle pollution during  
106 wintertime – a season with frequent occurrences of pollution episodes in Beijing was  
107 extensively investigated and the results highlighted the similar importance of SOA to  
108 SIA (Sun et al., 2013b;Sun et al., 2014;Zhang et al., 2014). However, the role of SOA  
109 in particulate pollution during periods with largely reduced anthropogenic activities is  
110 not well known yet (Huang et al., 2012). This study happened to take place in a month  
111 with the most important holiday in China, i.e., the Spring Festival. The source  
112 emissions (e.g., traffic and cooking) have significant changes due to a large reduction  
113 of population and anthropogenic activities in the city. This provides a unique  
114 opportunity to investigate how source changes affect aerosol chemistry including

---

115 primary emissions and secondary formation in Beijing. Although Huang et al. (2012)  
116 investigated such a holiday effect on aerosol composition and optical properties in  
117 Shanghai, the data analyses were limited by daily average composition measurements  
118 and also the significantly different meteorological conditions between holiday and  
119 non-holiday periods.

120 In this study, an Aerosol Chemical Speciation Monitor (ACSM) along with  
121 various collocated instruments was deployed in Beijing during February 2013. The  
122 chemical composition of submicron aerosol ( $PM_{10}$ ) from fireworks is quantified based  
123 on the highly time – resolved measurements of non-refractory submicron aerosol  
124 (NR- $PM_{10}$ ) species (organics, sulfate, nitrate, ammonium, chloride, and potassium) and  
125 black carbon. The impacts of fireworks on PM pollution during Chinese Lunar New  
126 Year (LNY), Lunar Fifth Day (LFD), and Lantern Festival (LF) are investigated, and  
127 the roles of secondary formation in PM pollution are elucidated. Further, the effects of  
128 reduced anthropogenic emissions on primary and secondary aerosols in the city are  
129 illustrated, which has significant implications for making air pollution control  
130 strategies in Beijing.

## 131 **2 Experimental**

### 132 **2.1 Sampling site**

133 The measurements in this study were conducted at the Institute of Atmospheric  
134 Physics (IAP), Chinese Academy of Sciences ( $39^{\circ}58'28''N$ ,  $116^{\circ}22'16''E$ ), an urban  
135 site located between the north third and fourth ring road in Beijing (Sun et al., 2012).  
136 Aerosol measurements were performed from 1 February to 1 March 2013 when three  
137 episodes with significant influences of fireworks, i.e., Lunar New Year (LNY), Lunar  
138 Fifth Day (LFD), and Lantern Festival (LF), were observed (Fig. 1). The

---

139 meteorological conditions during the measurement period are reported in Fig. 1.  
140 Winds at the ground surface were generally below  $2 \text{ m s}^{-1}$  and temperature averaged  
141  $0.6 \text{ }^\circ\text{C}$ . Relative humidity (RH) varied periodically with higher values generally  
142 associated with higher PM pollution.

## 143 **2.2 Aerosol sampling**

144 The chemical composition of NR-PM<sub>1</sub> including organics, sulfate, nitrate,  
145 ammonium, and chloride were measured *in situ* by the ACSM at an approximate  
146 15-min time intervals (Ng et al., 2011b). The ACSM has been widely used for  
147 long-term and routine aerosol particle composition measurements due to its  
148 robustness (Sun et al., 2012; Budisulistiorini et al., 2014; Petit et al., 2014) despite its  
149 lower sensitivity and mass resolution compared to previous versions of research-grade  
150 AMS (Jayne et al., 2000; DeCarlo et al., 2006). In this study, the ambient air was  
151 drawn inside the sampling room at a flow rate of  $3 \text{ L min}^{-1}$ , of which  $\sim 0.1 \text{ L min}^{-1}$  was  
152 sub-sampled into the ACSM and  $0.85 \text{ L min}^{-1}$  into a Cavity Attenuated Phase Shift  
153 Spectrometer (CAPS) particle extinction monitor (Massoli et al., 2010). A PM<sub>2.5</sub>  
154 cyclone (Model: URG-2000-30ED) was supplied in front of the sampling line to  
155 remove coarse particles with aerodynamic diameters larger than  $2.5 \text{ }\mu\text{m}$ . The aerosol  
156 particles were dried by a silica gel dryer (RH < 40%) before entering the ACSM and  
157 the CAPS. The ACSM was operated at a scan rate of  $500 \text{ ms amu}^{-1}$  for the mass  
158 spectrometer from  $m/z$  10 – 150. Because ACSM cannot detect refractory components,  
159 e.g., BC and mineral dust, a two-wavelength Aethalometer (Model AE22, Magee  
160 Scientific Corp.) was therefore used to measure refractory BC in PM<sub>2.5</sub>. The light  
161 extinction of dry fine particles ( $b_{\text{ext}}$ , 630 nm) was measured at 1 s time resolution with  
162 a precision ( $3 \sigma$ ) of  $1 \text{ M m}^{-1}$  by the CAPS monitor. In addition, the mass concentration

---

163 of PM<sub>2.5</sub> was determined by a heated Tapered Element Oscillating Microbalance,  
164 TEOM, and the collocated gaseous species (including CO, SO<sub>2</sub>, NO, NO<sub>x</sub> and O<sub>3</sub>)  
165 were measured by various gas analyzers (Thermo Scientific) at 1 min time resolution.  
166 A more detailed descriptions of aerosol and gas measurements were given in Sun et al.  
167 (2013b).

### 168 **2.3 ACSM data analysis**

169 The ACSM data were analyzed for the mass concentrations and chemical  
170 composition of NR-PM<sub>1</sub> using standard ACSM software (v 1.5.3.2) written within  
171 Igor Pro (WaveMetrics, Inc., Oregon USA). A composition-dependent collection  
172 efficiency (CE) recommended by Middlebrook et al.(2012),  $CE = \max(0.45, 0.0833$   
173  $+ 0.9167 \times \text{ANMF})$ , was used to account for the incomplete detection due to the  
174 particle bouncing effects (Matthew et al., 2008) and the influences caused by high  
175 mass fraction of ammonium nitrate (ANMF). Because aerosol particles were overall  
176 neutralized ( $\text{NH}_4^+_{\text{measured}}/\text{NH}_4^+_{\text{predicted}} = 1.01$ ,  $r^2 = 0.99$ ) and also dried before entering  
177 the ACSM, the effects of particle acidity and RH would be minor (Matthew et al.,  
178 2008;Middlebrook et al., 2012). The default relative ionization efficiencies (RIEs)  
179 except ammonium (RIE = 6.5) that was determined from the IE calibration were used  
180 in this study..Quantification of  $\text{K}^+$  is challenging for ACSM because of a large  
181 interference of organic  $\text{C}_3\text{H}_3^+$  at  $m/z$  39 and also uncertainties caused by surface  
182 ionization (Slowik et al., 2010). In this work, we found that  $m/z$  39 was tightly  
183 correlated with  $m/z$  43 that is completely organics during non-fireworks (NFW)  
184 periods ( $r^2 = 0.87$ , slope = 0.45, Fig. S1). However, higher ratios of  $m/z$  39/43 during  
185 FW periods were observed due to the elevated  $\text{K}^+$  signal from burning of fireworks.  
186 Assuming that  $m/z$  39 was primarily contributed by organics during NFW periods, the



---

187 excess  $m/z$  39 signal, i.e.,  $K^+$ , can then be estimated as  $m/z$  39 –  $m/z$  43  $\times$  0.45. The  
188  $^{41}K^+$  at  $m/z$  41 was calculated using an isotopic ratio of 0.0722, i.e.,  $^{41}K^+ = 0.0722 \times$   
189  $K^+$ . The  $K^+$  signal was converted to mass concentration with a RIE of 2.9 that was  
190 reported by Drewnick et al. (2006). It should be noted that the quantification of  $K^+$  in  
191 this study might have a large uncertainty because of the unknown RIE of  $K^+$  ( $RIE_K$ ).  
192 The  $RIE_K$  can vary a lot depending on the tuning of the spectrometer and the  
193 temperature of the vaporizer. For example, Slowik et al. (2010) reported a  $RIE_K = 10$   
194 based on the calibration of pure  $KNO_3$  particles using a ToF-AMS, which is much  
195 higher than the  $RIE_K = 2.9$  obtained from the comparisons of K/S from fireworks and  
196 AMS measurements (Drewnick et al., 2006). In addition, the stability of surface  
197 ionization (SI) and electron impact (EI) also affects  $RIE_K$ . We then checked the  
198 variations of the ratio of  $m/z$  39/ $m/z$  23 (two  $m/z$ 's with similar surface ionization  
199 issues). The average ratio of  $m/z$  39/23 during LFD and LF is 8.7 and 11.1,  
200 respectively, which is close to 9.0 during the NFW periods. The results suggest that  
201 the SI/EI ratio was relatively stable throughout the study. Because we didn't have  
202 collocated K measurement,  $RIE_K = 2.9$  that was estimated from fireworks was used in  
203 this study. The quantified  $K^+$  during LFD and LF on average contributed 4.5% and  
204 4.7% of  $PM_{10}$ , respectively, which is close to  $\sim 5\%$  ( $PM_{2.5}$ ) reported by Cheng et al.  
205 (2014). Also, the large contribution of  $K^+$  to  $PM_{10}$  (20.5%) during LNY, likely due to  
206 the intensified firework emissions (mainly firecrackers), is consistent with that (17.3%)  
207 observed during LNY 2014 in megacity Tianjin (Tian et al., 2014). Using  $RIE_K=10$   
208 will decrease the  $K^+$  concentration by a factor of more than 3, which appears to  
209 underestimate  $K^+$  a lot. Therefore,  $RIE_K = 2.9$  for the quantification of  $K^+$  in our study  
210 appear to be reasonable. The  $KCl^+$  ( $m/z$  74) and  $^{41}KCl^+/K^{37}Cl^+$  ( $m/z$  76) were  
211 estimated by the differences between the measured and PMF modeled  $m/z$  74 (Fig.

---

212 S2). Not surprisingly, the quantified  $\text{KCl}^+$  highly correlates with  $\text{K}^+$  ( $r^2 = 0.82$ , Fig.  
213 S2c). The chloride concentration was also biased at  $m/z$  35 during some periods (e.g.,  
214 LNY, Fig. S3), which is likely due to the interferences of  $\text{NaCl}$  from fireworks.  
215 Therefore,  $\text{Cl}^+$  ( $m/z$  35) was recalculated based on its correlation with  $m/z$  36 (mainly  
216  $\text{HCl}^+$  with negligible  $\text{C}_3^+$  and  $^{36}\text{Ar}$ ), i.e.,  $m/z$  35 =  $0.15 \times m/z$  36. The  $^{37}\text{Cl}^+$  was  
217 calculated using an isotopic ratio of 0.323, i.e.,  $^{37}\text{Cl}^+ = 0.323 \times ^{35}\text{Cl}^+$ . The comparison  
218 of the reconstructed chloride from the default values is shown in Fig. S3b.

219 The positive matrix factorization (PMF) with the algorithm of PMF2.exe in robust  
220 mode (Paatero and Tapper, 1994) was performed on organic aerosol (OA) mass  
221 spectra ( $m/z$  12 – 120) to resolve distinct OA components from different sources. The  
222 PMF results were evaluated with an Igor Pro-based PMF Evaluation Tool (PET, v  
223 2.04) (Ulbrich et al., 2009) following the procedures detailed in Zhang et al. (2011).  
224 After a careful evaluation of the spectral profiles, diurnal variations and correlations  
225 with external tracers, a 6-factor solution ( $Q/Q_{\text{exp}} = 4.3$ ) was chosen, yielding a  
226 hydrocarbon-like OA (HOA), a cooking OA (COA), a coal combustion OA (CCOA),  
227 and three oxygenated OA (OOA) components. Because of the absence of collocated  
228 measurements to validate the different OOA components, the three OOA components  
229 were recombined into one OOA component. The contributions of four OA factors  
230 were relatively stable across different  $f_{\text{peak}}$  values (average  $\pm 1\sigma$ ; min – max, Fig. S4):  
231 HOA ( $14 \pm 1.6\%$ ; 12 – 16%), COA ( $14 \pm 2.8\%$ ; 11 – 17%), CCOA ( $19 \pm 2.7\%$ ; 15 –  
232 22%), and OOA ( $51 \pm 1.7\%$ ; 49 – 55%). However, considering the mass spectra of OA  
233 factors at  $f_{\text{peak}} = -1$  presented the best correlation with those identified in winter  
234 2011-2012 ( $r^2 = 0.86 - 0.99$ , Fig. S5) (Sun et al., 2013b), the four OA factors with  
235  $f_{\text{peak}} = -1$  was chosen in this study. The HOA spectrum resembles to that identified

---

236 by PMF analysis of high resolution OA mass spectra in Beijing in January 2013  
237 (Zhang et al., 2014) which are both characterized pronounced  $m/z$  91 and 115.  
238 Although the CCOA spectrum doesn't present similar pronounced  $m/z$ 's (e.g., 77, 91,  
239 105, and 115) as that resolved at a rural site in Central Eastern China (Hu et al., 2013),  
240 it shows more similarity to that resolved in Beijing (Zhang et al., 2014). Also, CCOA  
241 correlates better with chloride with an importance source from coal combustion  
242 (Zhang et al., 2012) than HOA ( $r^2 = 0.41$  vs. 0.24), and also correlates well with  $m/z$   
243 60 ( $r^2 = 0.77$ , Fig. S6) a tracer  $m/z$  for biomass burning (Cubison et al., 2011). Note  
244 that better correlations between HOA+CCOA and BC ( $r^2 = 0.88$ ),  $\text{NO}_x$  ( $r^2 = 0.77$ ),  
245 and CO ( $r^2 = 0.63$ ) than HOA ( $r^2 = 0.36 - 0.47$ ) were observed in this study, which  
246 might suggest that coal combustion emissions are also important sources of CO, BC  
247 and  $\text{NO}_x$  during wintertime (Tian et al., 2008; Zhi et al., 2008).. Although COA didn't  
248 have external tracers to validate, it is very distinct as suggested by its unique diurnal  
249 patterns (two peaks corresponding to meal time) and high  $m/z$  55/57 ratio. Similar to  
250 our previous study (Sun et al., 2013b), the OOA shows a tight correlation with  $\text{NO}_3$   
251 ( $r^2 = 0.90$ ) and also a good correlation with  $\text{SO}_4^{2-} + \text{NO}_3^-$  ( $r^2 = 0.87$ ). The mass spectral  
252 profiles and time series of four OA factors are shown in Fig. S6.

253 No biomass burning OA (BBOA) was resolved in this study. One of the reasons is  
254 that BBOA was likely not an important component of OA (e.g., < 5%), which is  
255 unlikely to be resolved accurately by PMF (Ulbrich et al., 2009). Indeed, we didn't  
256 observe strong biomass burning influences throughout the study by checking the  
257 scatter plot of  $f_{60}$  vs.  $f_{44}$  (Fig. S7). We found that  $f_{60}$  vs.  $f_{44}$  in Fig. S7 is outside of the  
258 typical biomass burning region (Cubison et al., 2011) for most of the time during this  
259 study. Although the average  $f_{60}$  (0.42%) is slightly higher than the typical value of  $f_{60}$

---

260 (~0.3%) in the absence of biomass burning impact (DeCarlo et al., 2008;Ulbrich et al.,  
261 2009), it is also likely due to the short range of  $m/z$  (12 – 120) used for the calculation  
262 of  $f_{60}$ . A summary of other key diagnostic plots of the PMF solution are given in Fig.  
263 S8 and Fig. S9.

### 264 **3 Results and discussion**

#### 265 **3.1 Identification and quantification of fireworks events**

266 Burning of fireworks has been found to emit a large amount of  $K^+$ , which can be  
267 used to identify the FW events (Drewnick et al., 2006;Wang et al., 2007). As shown  
268 in Fig. 1 and Fig. 2, three FW events with significantly elevated  $K^+$  were observed on  
269 the days of Lunar New Year (LNY, 9-10 February), Lunar Fifth Day (LFD, 14  
270 February), and Lantern Festival (LF, 24 February), respectively. All three FW events  
271 started approximately at 18:00 and ended at midnight except LNY with a continuous  
272 FW impact until 4:00 on the second day (Fig. 2). Fig. 1 shows that the relative  
273 humidity was generally below 30% during LNY and LFD. While the wind speed at  
274 the ground surface remained consistently below  $2 \text{ m s}^{-1}$ , it was increased to  $\sim 4 \text{ m s}^{-1}$   
275 at the height of 100 m. Also note that there was a wind direction change in the middle  
276 of the two events. The meteorological conditions during LF were stagnant with wind  
277 speed generally below  $2 \text{ m s}^{-1}$  across different heights. The relative humidity was  $\sim 50\%$   
278 and the temperature averaged  $3.5^\circ\text{C}$ .

279 To estimate the contributions of fireworks, we first assume that the background  
280 concentration of each species has a linear variation during FW period. A linear fit was  
281 then performed on the 6 h data before and after FW events. The difference between  
282 the measured and the fitted value is assumed as the contribution from FW. The typical  
283 examples for estimating FW contributions are shown in Fig. S10. It should be noted

---

284 that this approach might significantly overestimate the FW contributions of primary  
285 species (e.g., HOA, COA, CCOA, and BC) that were largely enhanced during the  
286 typical FW periods (18:00 – 24:00) due to the increased local emissions (see Fig. S11  
287 for diurnal variations of aerosol species). However, it should have a minor impact on  
288 secondary species (e.g., SO<sub>4</sub>, NO<sub>3</sub>, and OOA) because of their relatively stable  
289 variations between 18:00-24:00. As shown in Fig.2, all aerosol species showed  
290 substantial increases from 15:00 to 21:00 on the day of LNY which coincidentally  
291 corresponded to a gradual change of wind direction. Therefore, regional transport  
292 might have played dominant roles for the evolution of chemical species during this  
293 period. For these reasons, only the FW contributions between 23:30, 9 February and  
294 3:30, 10 February when the meteorological conditions were stable were estimated.  
295 The FW contributions during LFD might also be overestimated due to the influences  
296 of regional transport as suggested by the wind direction change in the middle.

### 297 **3.2 Mass concentration and chemical composition of FW aerosols**

298 Figure 1 shows the time series of mass concentrations of PM<sub>1</sub>, PM<sub>2.5</sub>, and  
299 submicron aerosol species from 1 February to 1 March 2013. Because ACSM cannot  
300 measure the metals (e.g., Sr, Ba, Mg, etc.) that were significantly enhanced during  
301 FW periods (Wang et al., 2007; Vecchi et al., 2008), the PM<sub>1</sub> in this study refer to  
302 NR-PM<sub>1</sub> (= Org + SO<sub>4</sub> + NO<sub>3</sub> + NH<sub>4</sub> + Chl + K + KCl) + BC. The PM<sub>2.5</sub> showed three  
303 prominent FW peaks with the maximum concentration occurring at ~00:30 during  
304 LNY and ~21:30 during LFD and LF, respectively. The peak concentration of PM<sub>2.5</sub>  
305 during LNY (775 μg m<sup>-3</sup>) is more than 10 times higher than the China National  
306 Ambient Air Quality Standard (75 μg m<sup>-3</sup>, 24 h average). The average FW-PM<sub>2.5</sub> mass  
307 concentrations during three FW events all exceeded 100 μg m<sup>-3</sup>. These results suggest

---

308 that fireworks have large impacts on fine particle pollution, yet generally less than  
309 half day (approximately 10 h for LNY, and 6 h for LFD and LF). The  $PM_{10}$  also  
310 showed increases during the FW periods, yet not as significant as  $PM_{2.5}$ . In fact the  
311 correlation of  $PM_{10}$  versus  $PM_{2.5}$  shows much lower  $PM_{10}/PM_{2.5}$  (0.08 – 0.19) ratios  
312 during three FW events than that observed during NFW periods (0.90) (Fig. 3). One  
313 of the reasons is likely due to the mineral dust component and metals from fireworks  
314 that ACSM did not measure. However, the ACSM un-detected metals (e.g., Mg, Sr,  
315 and Ba) that are largely enhanced during FW periods generally contribute a small  
316 fraction of PM (<2%) (Wang et al., 2007; Vecchi et al., 2008; Kong et al., 2014).  
317 Therefore, our results might suggest that a large fraction of aerosol particles from the  
318 burning of fireworks was emitted in the size range of 1 – 2.5  $\mu m$ . Consistently,  
319 Vecchi et al. (2008) found the best correlation between the fireworks tracer, Sr, and  
320 the particles between 700-800 nm (mobility diameter,  $D_m$ ) which is approximately  
321 equivalent to 1.9 – 2.2  $\mu m$  in  $D_{va}$  (vacuum aerodynamic diameter,  $D_{va}$ ) with a density  
322 of 2.7  $g\ cm^{-3}$  (Zhang et al., 2010).

323 Figure 4 shows the average chemical composition of  $PM_{10}$  and OA from  
324 fireworks and also the background composition during LNY, LFD and LF. The  
325 background  $PM_{10}$  during LNY and LFD showed typical characteristics of clean  
326 periods with high fraction of organics (> ~50%) (Sun et al., 2012; Sun et al., 2013b),  
327 whereas that during LF was dominated by SIA (52%). As a comparison, organics  
328 constituted the major fraction of FW- $PM_{10}$ , contributing 44 – 55% on average. During  
329 LNY, FW exerted large impacts on potassium and chloride whose contributions were  
330 elevated to 21% and 15% of  $PM_{10}$ , respectively, from less than 7% (Chl) in the  
331 background aerosols. The large increases of potassium and chloride were also

---

332 observed during LFD and LF, and previous studies in Beijing (Wang et al.,  
333 2007; Cheng et al., 2014). As shown in Fig. 4, FW also emitted a considerable amount  
334 of sulfate, accounting for 7% - 14% of PM<sub>1</sub>. Sulfate correlated strongly with SO<sub>2</sub>  
335 during all three FW events ( $r^2 = 0.49 - 0.92$ ). Given that the relative humidity was low,  
336 < 30% during LNY and LFD, and ~ 50% during LF, aqueous-phase oxidation of SO<sub>2</sub>  
337 depending on liquid water content could not play significant roles for the sulfate  
338 formation (Sun et al., 2013a). Therefore, sulfate in FW-PM<sub>1</sub> was mainly from the  
339 direction emissions of FW. Compared to sulfate, FW appeared to show minor impacts  
340 on nitrate, for example, 4% and 2% during LNY and LF, respectively. Although  
341 nitrate contributed 12% of FW-PM<sub>1</sub> during LFD, most of it was likely from regional  
342 transport as supported by synchronous increases of all aerosol species associated with  
343 a wind direction change in the middle (Fig. 2).

344       The OOA contributed dominantly to OA during LNY, which is 79% on average  
345 (Fig. 4a). As shown in Fig. 5, the mass spectrum of FW-organics is highly similar to  
346 that of low-volatility OOA (LV-OOA,  $r^2 = 0.94$ ;  $r^2 = 0.89$  by excluding  $m/z$  18 and  
347  $m/z$  44) (Ng et al., 2011a) indicating that the FW-organics is likely emitted in  
348 secondary. Consistently, Drewnick et al. (2006) also found large enhancements of the  
349 OOA-related  $m/z$ 's (e.g.,  $m/z$  44) during New Year's fireworks, but the HOA-related  
350  $m/z$ 's (e.g.,  $m/z$  57) are not significant contributors to FW organics. OOA accounted  
351 for a much smaller fraction of OA during LF (28%) due to the large contributions of  
352 POA components (72%). Although the OOA contributions varied during three FW  
353 events, their absolute concentrations were relatively close ranging from 5.8 to 7.9  $\mu\text{g}$   
354  $\text{m}^{-3}$ . It should be noted that our approach might overestimate the POA components in  
355 FW-OA because of the influences of NFW sources, in particular during the FW

---

356 period of LF when the local HOA, COA, and CCOA happened to have large increases.  
357 By excluding the POA components in FW-OA, FW on average contributed 15 – 19  
358  $\mu\text{g m}^{-3}$   $\text{PM}_1$  during three FW events.

### 359 **3.3 Secondary aerosol and PM pollution**

360 The  $\text{PM}_1$  (NR- $\text{PM}_1$  + BC) varied largely across the entire study with daily average  
361 mass concentration ranging from 9.1 to 169  $\mu\text{g m}^{-3}$ . The average  $\text{PM}_1$  mass  
362 concentration was 80 ( $\pm 68$ )  $\mu\text{g m}^{-3}$ , which is approximately 20% higher than that  
363 observed during winter 2011-2012 (Sun et al., 2013b). Organics composed the major  
364 fraction of  $\text{PM}_1$  accounting for 43%, followed by nitrate (22%), sulfate (14%),  
365 ammonium (13%), BC (5%) and chloride (3%). The OA composition was dominated  
366 by OOA (53%) with the rest being POA. Compared to winter 2011-2012 (Sun et al.,  
367 2013b), this study showed significantly enhanced OOA (53% vs. 31%) and secondary  
368 nitrate (22% vs. 16%), indicating that secondary formation have played important  
369 roles in the formation of pollution episodes.

370 Figure 1d shows that submicron aerosol species alternated routinely between  
371 pollution events (PEs) and clean periods (CPs) throughout the entire study. The PEs  
372 generally lasted  $\sim 1 - 2$  days except the one on 23 – 28 February that lasted more than  
373 5 days, whereas the CPs were shorter, generally less than 1 day. In total, 9 PEs and 9  
374 CPs were identified in this study (Fig. 1). A statistics of the mass concentrations and  
375 mass fractions of aerosol species during 9 PEs is presented in Fig. 6. The average  $\text{PM}_1$   
376 mass concentration ranged 68 – 179  $\mu\text{g m}^{-3}$  during PEs with the total secondary  
377 particulate matter (SPM = OOA +  $\text{SO}_4$  +  $\text{NO}_3$  +  $\text{NH}_4$ ) accounting for 63 – 82%. The  
378 average mass concentration of SPM for the 9 PEs was 86 ( $\pm 32$ )  $\mu\text{g m}^{-3}$ , which is  
379 nearly 3 times that of primary PM (PPM = HOA + COA + CCOA + BC + Chl) (30



---

380  $\pm 9.5 \mu\text{g m}^{-3}$ ). SPM consistently dominated  $\text{PM}_{10}$  across different PM levels (69 – 75%),  
381 but generally with higher contributions (up to 81%) during daytime (Fig. 7b). The  
382 diurnal cycle of SPM presented a gradual increase from 50 to  $70 \mu\text{g m}^{-3}$  between  
383 10:00 – 20:00, indicating evident photochemical production of secondary species  
384 during daytime. It should be also noted that all secondary species showed  
385 ubiquitously higher mass concentrations than those of primary species (Fig. 6a).

386       The SOA generally contributed more than 50% to OA with an average of 55%  
387 during PEs except the episode on 3 February (35%). It's interesting to note that the  
388 contribution of POA increased as a function of organic loadings which varied from  
389  $\sim 35\%$  to 63% when organics was above  $80 \mu\text{g m}^{-3}$  (Fig. 7c). Such behavior is mainly  
390 caused by the enhanced CCOA at high organic mass loadings, which was also  
391 observed during winter 2011 – 2012 (Sun et al., 2013b). These results suggest that  
392 POA played more important roles than SOA in PM pollution during periods with high  
393 organic mass loadings (e.g.,  $> 60 \mu\text{g m}^{-3}$ ). In fact, POA showed even higher mass  
394 concentration than OOA at nighttime (0:00 – 8:00) due to the intensified local  
395 emissions, e.g., coal combustion for heating. Despite this, the role of POA in PM  
396 pollution was compensated by the elevated secondary inorganic species as a function  
397 of PM loadings (Fig. 7a) leading to the consistently dominant SPM across different  
398 pollution levels. Figure 8a shows an evidently lower contribution of organics to  $\text{PM}_{10}$   
399 during PEs than CPs. The elevated secondary inorganic species during PEs were  
400 closely related to the increase of RH (Fig. 1). For example, during the pollution  
401 episode on 3 February, the sulfate concentration increased rapidly and became the  
402 major inorganic species when RH was increased from  $\sim 60\%$  to  $> 90\%$ . The gaseous  
403  $\text{SO}_2$  showed a corresponding decrease indicating aqueous-phase processing of  $\text{SO}_2$  to

---

404 form sulfate, consistent with our previous conclusion that aqueous-phase processing  
405 could contribute more than 50% of sulfate production during winter 2011-2012 (Sun  
406 et al., 2013a).

407 The compositional differences between PEs and CPs also led to different mass  
408 extinction efficiency (MEE, 630 nm) of PM<sub>1</sub> (Fig. 8b). The higher MEE (6.4 m<sup>2</sup> g<sup>-1</sup>)  
409 during PEs than CPs (4.4 m<sup>2</sup> g<sup>-1</sup>) is primarily due to the enhanced secondary species,  
410 and also likely the increases of aerosol particle sizes although we don't have size data  
411 to support it. Similar increases of mass scattering efficiency from clean periods to  
412 relatively polluted conditions were also observed previously in Beijing and Shanghai  
413 (Jung et al., 2009;Huang et al., 2013). It should be noted that the MEE of PM<sub>1</sub> in this  
414 study refers to PM<sub>2.5</sub> *b*<sub>ext</sub>/PM<sub>1</sub>. Considering that PM<sub>1</sub> on average contributes ~60-70%  
415 of PM<sub>2.5</sub> in Beijing (Sun et al., 2012;Sun et al., 2013b), the real MEE of PM<sub>1</sub> during  
416 PEs and CPs would be ~3.8 - 4.5 and ~2.6 - 3.1 m<sup>2</sup> g<sup>-1</sup>, respectively.

### 417 **3.4 Holiday Effects on PM Pollution**

418 Figure 9 shows a comparison of aerosol species, gaseous species, and  
419 meteorological parameters between holiday (HD) and non-holiday (NHD) periods.  
420 The official holiday for the Spring Festival was 9 – 15 February. However, we noted a  
421 large decrease of cooking aerosols from 7 February until 19 February (Fig. S6b),  
422 whose emissions were expected to be stable under similar meteorological conditions.  
423 The decrease of COA was likely due to the reduction of the number of population in  
424 Beijing, which agreed with the fact that most migrants from outside Beijing were  
425 leaving for hometown before the official holiday. Therefore, 7 – 19 February was  
426 used as a longer holiday for a comparison. It was estimated that approximately half of  
427 population (9 million) left Beijing before the Spring Festival

---

428 ([http://news.xinhuanet.com/yzyd/local/20130208/c\\_114658765.htm](http://news.xinhuanet.com/yzyd/local/20130208/c_114658765.htm)). Such a great  
429 reduction in human activities would exert a large impact on aerosol composition and  
430 sources in the city during holidays. To better investigate the HD effects on PM  
431 pollution, the data shown in Fig. 9 excluded the CPs marked in Fig. 1. The data with  
432 the CPs included are presented in Fig. S12.

433 The differences between HD and NHD for primary species varied largely among  
434 different species. COA showed the largest reduction (69%) among aerosol species  
435 with the average concentration decreasing from  $5.8 \mu\text{g m}^{-3}$  during NHD to  $1.8 \mu\text{g m}^{-3}$   
436 during HD. The contribution of COA to OA showed a corresponding decrease from  
437 12% to 4%. Given the similar meteorological conditions between HD and NHD, e.g.,  
438 RH (46% vs. 52%) and wind speed ( $1.3 \text{ m s}^{-1}$  vs.  $1.2 \text{ m s}^{-1}$ ), the reduction of COA  
439 clearly indicated a large decrease of population and the number of restaurants opened  
440 during HD. The CCOA showed approximately 30% reduction during HD, and its  
441 contribution to OA decreased from 23% to 18%. Not surprisingly, chloride showed a  
442 similar reduction as CCOA because it was primarily from coal combustion emissions  
443 during wintertime (Sun et al., 2013b). Figure 9 also shows a significant reduction  
444 (54%) for NO indicating much less traffic emissions in the city during HD. The HOA,  
445 however, even showed a slight increase during HD, which appeared to contradict with  
446 the reduction of two combustion-related tracers, BC and CO (~20%). This can be  
447 explained by the fact that coal combustion is a large source of BC and CO during  
448 heating season (Tian et al., 2008; Zhi et al., 2008). Consistently, BC and CO showed  
449 relatively similar reductions to CCOA. Therefore, the minor variation of HOA might  
450 indicate that the number of heavy-duty vehicles and diesel trucks that dominated  
451 HOA emissions (Massoli et al., 2012; Hayes et al., 2013) remained little change during

---

452 HD period although that of gasoline vehicles was largely decreased. It should be  
453 noted that HOA showed a large peak on 9 February – the first day of the official  
454 holiday (Fig. S6b) when more traffic emissions were expected due to many people  
455 leaving for hometown. After that, HOA showed slightly lower concentration during  
456 11 – 17 February than other periods. In fact, the average HOA showed a slight  
457 reduction (~5%) during the long holiday period (7 – 19 February) suggesting a small  
458 holiday effect on HOA reduction. Together, the total primary aerosol species (PPM)  
459 showed an average reduction of 22% because of holiday effects.

460 Nitrate showed the largest reduction among secondary species by 22% during HD,  
461 primarily due to a reduction of its precursors NO and NO<sub>2</sub>. The results suggest that  
462 reducing traffic emissions would help mitigate the nitrate pollution in the city.  
463 Compared to nitrate, sulfate showed minor changes (2%) between HD and NHD, and  
464 OOA even showed a slight increase (6%) during HD. One of the reasons is that  
465 secondary sulfate and OOA were mainly formed over regional scale and less affected  
466 by local production, consistent with their relatively flat diurnal cycles (Fig. S11).  
467 Ammonium showed a reduction between nitrate and sulfate because ammonium  
468 mainly existed in the form of (NH<sub>4</sub>)<sub>2</sub>SO<sub>4</sub> and NH<sub>4</sub>NO<sub>3</sub>. Overall, secondary species  
469 showed generally lower reductions than primary species with the total secondary  
470 species (SPM) showing an average reduction of 9% during HD. The joint reductions  
471 of PPM and SPM led to an average reduction of 13% for PM<sub>1</sub> during HD. However,  
472 these reductions did not help alleviate the fine particle pollution during HD. The  
473 PM<sub>2.5</sub> excluding FW impacts even showed 27% increase from 96 μg m<sup>-3</sup> during NHD  
474 to 122 μg m<sup>-3</sup> during HD. One possible reason is likely due to the increases of aerosol  
475 species in the size range of 1 – 2.5 μm during HD period. The longer holiday (LHD, 7

---

476 – 19 February) showed similar influences on both primary and secondary species as  
477 the official holiday (9 – 15 February). COA, CCOA, and NO are the three species  
478 with the largest reductions during LHD (> 50%). However, HOA, SO<sub>4</sub>, OOA, and  
479 PM<sub>2.5</sub> showed rather small changes (< ±7%). Therefore, results in this study suggest  
480 that controlling the primary source emissions, e.g., cooking and traffic emissions in  
481 the city can reduce the primary particles largely, yet has limited effects on secondary  
482 species and the total fine particle mass. One of the reasons is because the severe PM  
483 pollution in Beijing is predominantly contributed by secondary species (see  
484 discussions in section 3.3) that are formed over regional scales. Reducing the primary  
485 source emissions in local areas would have limited impacts on mitigation of air  
486 pollution in the city. Similarly, Guo et al. (2013) reported a large reduction of primary  
487 organic carbon (OC) from traffic emissions and coal combustion during the 2008  
488 Olympic Summer Games when traffic restrictions and temporary closure of factories  
489 were implemented. However, secondary OC was not statistically different between  
490 controlled and non-controlled periods. Our results highlight the importance of  
491 implementing joint efforts over regional scales for air pollution control in north  
492 China.

#### 493 **4 Conclusions**

494 We have characterized the aerosol particle composition and sources during the  
495 Chinese Spring Festival in 2013. The average PM<sub>1</sub> mass concentration was 80 (±68)  
496 μg m<sup>-3</sup> for the entire study with organics being the major fraction (43%). Nine  
497 pollution events and nine clean periods with substantial compositional differences  
498 were observed. The secondary particulate matter (= SOA+ sulfate + nitrate +  
499 ammonium) played a dominant role for the PM pollution during nine PEs. The

---

500 contributions of SPM to PM<sub>1</sub> varied from 63% to 82% with SOA on average  
501 accounting for ~55% of OA. As a result, the average mass extinction efficiency of  
502 PM<sub>1</sub> during PEs (6.4 m<sup>2</sup> g<sup>-1</sup>) was higher than that during CPs (4.4 m<sup>2</sup> g<sup>-1</sup>). Three FW  
503 events, i.e., LNY, LFD, and LF, were identified, which showed significant and  
504 short-term impacts on fine particles, and non-refractory potassium, chloride, and  
505 sulfate in PM<sub>1</sub>. The FW also exerted a large impact on organics that presented mainly  
506 in secondary as indicated by its similar mass spectrum to that of oxygenated OA. The  
507 holiday effects on aerosol composition and sources were also investigated by  
508 comparing the differences between holiday and non-holiday periods. The changes of  
509 anthropogenic source emissions during the holiday showed large impacts on reduction  
510 of cooking OA (69%), nitrogen monoxide (54%), and coal combustion OA (28%) in  
511 the city, yet presented much smaller influences on secondary species. The average  
512 SOA and the total PM<sub>2.5</sub> even increased slightly during the holiday period. Results  
513 here have significant implications that controlling the local primary source emissions,  
514 e.g., cooking and traffic activities, might have limited effects on improving air quality  
515 during polluted days when SPM from regional transport dominated aerosol  
516 composition for most of time. Our results also highlight the importance of  
517 implementing joint measures over regional scales for mitigation of air pollution in  
518 megacity Beijing.

519

## 520 **Acknowledgements**

521 This work was supported by the National Key Project of Basic Research  
522 (2014CB447900), the Strategic Priority Research Program (B) of the Chinese  
523 Academy of Sciences (Grant No. XDB05020501), and the National Natural Science

---

524 Foundation of China (41175108). We thank Huabin Dong, Hongyan Chen, and Zhe  
525 Wang's help in data collection, and also the Technical and Service Center, Institute of  
526 Atmospheric Physics, Chinese Academy of Sciences for providing meteorological  
527 data.

528

## 529 **References**

- 530 Budisulistiorini, S. H., Canagaratna, M. R., Croteau, P. L., Baumann, K., Edgerton, E. S.,  
531 Kollman, M. S., Ng, N. L., Verma, V., Shaw, S. L., Knipping, E. M., Worsnop, D. R.,  
532 Jayne, J. T., Weber, R. J., and Surratt, J. D.: Intercomparison of an Aerosol Chemical  
533 Speciation Monitor (ACSM) with ambient fine aerosol measurements in downtown  
534 Atlanta, Georgia, *Atmos. Meas. Tech.*, 7, 1929-1941, 10.5194/amt-7-1929-2014, 2014.
- 535 Chan, C. K., and Yao, X.: Air pollution in mega cities in China, *Atmos. Environ.*, 42, 1-42,  
536 DOI: 10.1016/j.atmosenv.2007.09.003, 2008.
- 537 Cheng, Y., Engling, G., He, K.-b., Duan, F.-k., Du, Z.-y., Ma, Y.-l., Liang, L.-l., Lu, Z.-f., Liu,  
538 J.-m., Zheng, M., and Weber, R. J.: The characteristics of Beijing aerosol during two  
539 distinct episodes: Impacts of biomass burning and fireworks, *Environ. Pollut.*, 185,  
540 149-157, <http://dx.doi.org/10.1016/j.envpol.2013.10.037>, 2014.
- 541 Cubison, M. J., Ortega, A. M., Hayes, P. L., Farmer, D. K., Day, D., Lechner, M. J., Brune,  
542 W. H., Apel, E., Diskin, G. S., Fisher, J. A., Fuelberg, H. E., Hecobian, A., Knapp, D. J.,  
543 Mikoviny, T., Riemer, D., Sachse, G. W., Sessions, W., Weber, R. J., Weinheimer, A. J.,  
544 Wisthaler, A., and Jimenez, J. L.: Effects of aging on organic aerosol from open biomass  
545 burning smoke in aircraft and laboratory studies, *Atmos. Chem. Phys.*, 11, 12049-12064,  
546 10.5194/acp-11-12049-2011, 2011.
- 547 DeCarlo, P. F., Kimmel, J. R., Trimborn, A., Northway, M. J., Jayne, J. T., Aiken, A. C.,  
548 Gonin, M., Fuhrer, K., Horvath, T., Docherty, K. S., Worsnop, D. R., and Jimenez, J. L.:  
549 Field-Deployable, High-Resolution, Time-of-Flight Aerosol Mass Spectrometer, *Anal.*  
550 *Chem.*, 78, 8281-8289, 2006.
- 551 DeCarlo, P. F., Dunlea, E. J., Kimmel, J. R., Aiken, A. C., Sueper, D., Crouse, J., Wennberg,  
552 P. O., Emmons, L., Shinozuka, Y., Clarke, A., Zhou, J., Tomlinson, J., Collins, D. R.,  
553 Knapp, D., Weinheimer, A. J., Montzka, D. D., Campos, T., and Jimenez, J. L.: Fast  
554 airborne aerosol size and chemistry measurements above Mexico City and Central  
555 Mexico during the MILAGRO campaign, *Atmos. Chem. Phys.*, 8, 4027-4048, 2008.
- 556 DeCarlo, P. F., Ulbrich, I. M., Crouse, J., de Foy, B., Dunlea, E. J., Aiken, A. C., Knapp, D.,  
557 Weinheimer, A. J., Campos, T., Wennberg, P. O., and Jimenez, J. L.: Investigation of the  
558 sources and processing of organic aerosol over the Central Mexican Plateau from aircraft  
559 measurements during MILAGRO, *Atmos. Chem. Phys.*, 10, 5257-5280,  
560 10.5194/acp-10-5257-2010, 2010.

---

561 Drewnick, F., Hings, S. S., Curtius, J., Eerdekens, G., and Williams, J.: Measurement of fine  
562 particulate and gas-phase species during the New Year's fireworks 2005 in Mainz,  
563 Germany, *Atmos. Environ.*, 40, 4316-4327, 10.1016/j.atmosenv.2006.03.040, 2006.

564 Duan, F. K., He, K. B., Ma, Y. L., Yang, F. M., Yu, X. C., Cadle, S. H., Chan, T., and  
565 Mulawa, P. A.: Concentration and chemical characteristics of PM<sub>2.5</sub> in Beijing, China:  
566 2001–2002, *Sci. Total Environ.*, 355, 264-275, 10.1016/j.scitotenv.2005.03.001, 2006.

567 Feng, J., Sun, P., Hu, X., Zhao, W., Wu, M., and Fu, J.: The chemical composition and  
568 sources of PM<sub>2.5</sub> during the 2009 Chinese New Year's holiday in Shanghai, *Atmospheric*  
569 *Research*, 118, 435-444, <http://dx.doi.org/10.1016/j.atmosres.2012.08.012>, 2012.

570 Godri, K. J., Green, D. C., Fuller, G. W., Dall'Osto, M., Beddows, D. C., Kelly, F. J.,  
571 Harrison, R. M., and Mudway, I. S.: Particulate oxidative burden associated with firework  
572 activity, 21, 8295-8301 pp., 2010.

573 Guo, S., Hu, M., Wang, Z. B., Slanina, J., and Zhao, Y. L.: Size-resolved aerosol  
574 water-soluble ionic compositions in the summer of Beijing: implication of regional  
575 secondary formation, *Atmos. Chem. Phys.*, 10, 947-959, 10.5194/acp-10-947-2010, 2010.

576 Guo, S., Hu, M., Guo, Q., Zhang, X., Schauer, J. J., and Zhang, R.: Quantitative evaluation of  
577 emission controls on primary and secondary organic aerosol sources during Beijing 2008  
578 Olympics, *Atmos. Chem. Phys.*, 13, 8303-8314, 10.5194/acp-13-8303-2013, 2013.

579 Hayes, P. L., Ortega, A. M., Cubison, M. J., Froyd, K. D., Zhao, Y., Cliff, S. S., Hu, W. W.,  
580 Toohey, D. W., Flynn, J. H., Lefer, B. L., Grossberg, N., Alvarez, S., Rappenglück, B.,  
581 Taylor, J. W., Allan, J. D., Holloway, J. S., Gilman, J. B., Kuster, W. C., de Gouw, J. A.,  
582 Massoli, P., Zhang, X., Liu, J., Weber, R. J., Corrigan, A. L., Russell, L. M., Isaacman, G.,  
583 Worton, D. R., Kreisberg, N. M., Goldstein, A. H., Thalman, R., Waxman, E. M.,  
584 Volkamer, R., Lin, Y. H., Surratt, J. D., Kleindienst, T. E., Offenberg, J. H., Dusanter, S.,  
585 Griffith, S., Stevens, P. S., Brioude, J., Angevine, W. M., and Jimenez, J. L.: Organic  
586 aerosol composition and sources in Pasadena, California during the 2010 CalNex  
587 campaign, *Journal of Geophysical Research: Atmospheres*, 118, 9233–9257,  
588 10.1002/jgrd.50530, 2013.

589 He, L.-Y., Huang, X.-F., Xue, L., Hu, M., Lin, Y., Zheng, J., Zhang, R., and Zhang, Y.-H.:  
590 Submicron aerosol analysis and organic source apportionment in an urban atmosphere in  
591 Pearl River Delta of China using high-resolution aerosol mass spectrometry, *J. Geophys.*  
592 *Res.*, 116, D12304, 10.1029/2010jd014566, 2011.

593 Hu, W. W., Hu, M., Yuan, B., Jimenez, J. L., Tang, Q., Peng, J. F., Hu, W., Shao, M., Wang,  
594 M., Zeng, L. M., Wu, Y. S., Gong, Z. H., Huang, X. F., and He, L. Y.: Insights on organic  
595 aerosol aging and the influence of coal combustion at a regional receptor site of central  
596 eastern China, *Atmos. Chem. Phys.*, 13, 10095-10112, 10.5194/acp-13-10095-2013,  
597 2013.

598 Huang, K., Zhuang, G., Lin, Y., Wang, Q., Fu, J. S., Zhang, R., Li, J., Deng, C., and Fu, Q.:  
599 Impact of anthropogenic emission on air quality over a megacity – revealed from an  
600 intensive atmospheric campaign during the Chinese Spring Festival, *Atmos. Chem. Phys.*,  
601 12, 11631-11645, 10.5194/acp-12-11631-2012, 2012.

602 Huang, R.-J., Zhang, Y., Bozzetti, C., Ho, K.-F., Cao, J.-J., Han, Y., Daellenbach, K. R.,  
603 Slowik, J. G., Platt, S. M., Canonaco, F., Zotter, P., Wolf, R., Pieber, S. M., Bruns, E. A.,



---

604 Crippa, M., Ciarelli, G., Piazzalunga, A., Schwikowski, M., Abbaszade, G.,  
605 Schnelle-Kreis, J., Zimmermann, R., An, Z., Szidat, S., Baltensperger, U., Haddad, I. E.,  
606 and Prevot, A. S. H.: High secondary aerosol contribution to particulate pollution during  
607 haze events in China, *Nature*, advance online publication, 10.1038/nature13774, 2014.

608 Huang, X. F., He, L. Y., Hu, M., Canagaratna, M. R., Sun, Y., Zhang, Q., Zhu, T., Xue, L.,  
609 Zeng, L. W., Liu, X. G., Zhang, Y. H., Jayne, J. T., Ng, N. L., and Worsnop, D. R.:  
610 Highly time-resolved chemical characterization of atmospheric submicron particles  
611 during 2008 Beijing Olympic Games using an Aerodyne High-Resolution Aerosol Mass  
612 Spectrometer, *Atmos. Chem. Phys.*, 10, 8933-8945, 10.5194/acp-10-8933-2010, 2010.

613 Huang, Y., Li, L., Li, J., Wang, X., Chen, H., Chen, J., Yang, X., Gross, D. S., Wang, H.,  
614 Qiao, L., and Chen, C.: A case study of the highly time-resolved evolution of aerosol  
615 chemical and optical properties in urban Shanghai, China, *Atmos. Chem. Phys.*, 13,  
616 3931-3944, 10.5194/acp-13-3931-2013, 2013.

617 Jayne, J. T., Leard, D. C., Zhang, X., Davidovits, P., Smith, K. A., Kolb, C. E., and Worsnop,  
618 D. R.: Development of an aerosol mass spectrometer for size and composition analysis of  
619 submicron particles, *Aerosol Sci. Tech.*, 33, 49-70, 2000.

620 Jung, J., Lee, H., Kim, Y. J., Liu, X., Zhang, Y., Hu, M., and Sugimoto, N.: Optical properties  
621 of atmospheric aerosols obtained by in situ and remote measurements during 2006  
622 Campaign of Air Quality Research in Beijing (CAREBeijing-2006), *J. Geophys. Res.*,  
623 114, D00G02, 10.1029/2008jd010337, 2009.

624 Kong, S., Li, L., Li, X., Yin, Y., Chen, K., Liu, D., Yuan, L., Zhang, Y., Shan, Y., and Ji, Y.:  
625 The impacts of fireworks burning at Chinese Spring Festival on air quality and human  
626 health: insights of tracers, source evolution and aging processes, *Atmos. Chem. Phys.*  
627 *Discuss.*, 14, 28609-28655, 10.5194/acpd-14-28609-2014, 2014.

628 Li, W., Shi, Z., Yan, C., Yang, L., Dong, C., and Wang, W.: Individual metal-bearing  
629 particles in a regional haze caused by firecracker and firework emissions, *Sci. Total*  
630 *Environ.*, 443, 464-469, <http://dx.doi.org/10.1016/j.scitotenv.2012.10.109>, 2013.

631 Liu, X. G., Li, J., Qu, Y., Han, T., Hou, L., Gu, J., Chen, C., Yang, Y., Liu, X., Yang, T.,  
632 Zhang, Y., Tian, H., and Hu, M.: Formation and evolution mechanism of regional haze: a  
633 case study in the megacity Beijing, China, *Atmos. Chem. Phys.*, 13, 4501-4514,  
634 10.5194/acp-13-4501-2013, 2013.

635 Massoli, P., Keibian, P. L., Onasch, T. B., Hills, F. B., and Freedman, A.: Aerosol Light  
636 Extinction Measurements by Cavity Attenuated Phase Shift (CAPS) Spectroscopy:  
637 Laboratory Validation and Field Deployment of a Compact Aerosol Particle Extinction  
638 Monitor, *Aerosol Sci. Tech.*, 44, 428-435, 10.1080/02786821003716599, 2010.

639 Massoli, P., Fortner, E. C., Canagaratna, M. R., Williams, L. R., Zhang, Q., Sun, Y., Schwab,  
640 J. J., Trimborn, A., Onasch, T. B., Demerjian, K. L., Kolb, C. E., Worsnop, D. R., and  
641 Jayne, J. T.: Pollution Gradients and Chemical Characterization of Particulate Matter  
642 from Vehicular Traffic Near Major Roadways: Results from the 2009 Queens College Air  
643 Quality Study in NYC, *Aerosol Sci. Tech.*, 46, 1201-1218,  
644 10.1080/02786826.2012.701784, 2012.

645 Matsui, H., Koike, M., Kondo, Y., Takegawa, N., Kita, K., Miyazaki, Y., Hu, M., Chang, S.  
646 Y., Blake, D. R., Fast, J. D., Zaveri, R. A., Streets, D. G., Zhang, Q., and Zhu, T.: Spatial

---

647 and temporal variations of aerosols around Beijing in summer 2006: Model evaluation  
648 and source apportionment, *J. Geophys. Res.*, 114, D00G13, 10.1029/2008jd010906, 2009.

649 Matthew, B. M., Middlebrook, A. M., and Onasch, T. B.: Collection Efficiencies in an  
650 Aerodyne Aerosol Mass Spectrometer as a Function of Particle Phase for Laboratory  
651 Generated Aerosols, *Aerosol Sci. Tech.*, 42, 884 - 898, 2008.

652 Middlebrook, A. M., Bahreini, R., Jimenez, J. L., and Canagaratna, M. R.: Evaluation of  
653 Composition-Dependent Collection Efficiencies for the Aerodyne Aerosol Mass  
654 Spectrometer using Field Data, *Aerosol Sci. Tech.*, 46, 258-271, 2012.

655 Molina, M. J., and Molina, L. T.: Megacities and atmospheric pollution, *J. Air Waste Manage.*  
656 *Assoc.*, 54, 644–680, 2004.

657 Moreno, T., Querol, X., Alastuey, A., Cruz Minguillón, M., Pey, J., Rodriguez, S., Vicente  
658 Miró, J., Felis, C., and Gibbons, W.: Recreational atmospheric pollution episodes:  
659 Inhalable metalliferous particles from firework displays, *Atmos. Environ.*, 41, 913-922,  
660 <http://dx.doi.org/10.1016/j.atmosenv.2006.09.019>, 2007.

661 Ng, N. L., Canagaratna, M. R., Jimenez, J. L., Zhang, Q., Ulbrich, I. M., and Worsnop, D. R.:  
662 Real-Time Methods for Estimating Organic Component Mass Concentrations from  
663 Aerosol Mass Spectrometer Data, *Environ. Sci. Technol.*, 45, 910-916,  
664 10.1021/es102951k, 2011a.

665 Ng, N. L., Herndon, S. C., Trimborn, A., Canagaratna, M. R., Croteau, P. L., Onasch, T. B.,  
666 Sueper, D., Worsnop, D. R., Zhang, Q., Sun, Y. L., and Jayne, J. T.: An Aerosol  
667 Chemical Speciation Monitor (ACSM) for Routine Monitoring of the Composition and  
668 Mass Concentrations of Ambient Aerosol, *Aerosol Sci. Tech.*, 45, 770 - 784, 2011b.

669 Paatero, P., and Tapper, U.: Positive matrix factorization: A non-negative factor model with  
670 optimal utilization of error estimates of data values, *Environmetrics*, 5, 111-126, 1994.

671 Petit, J. E., Favez, O., Sciare, J., Canonaco, F., Croteau, P., Močnik, G., Jayne, J., Worsnop,  
672 D., and Leoz-Garziandia, E.: Submicron aerosol source apportionment of wintertime  
673 pollution in Paris, France by double positive matrix factorization (PMF2) using an aerosol  
674 chemical speciation monitor (ACSM) and a multi-wavelength Aethalometer, *Atmos.*  
675 *Chem. Phys.*, 14, 13773-13787, 10.5194/acp-14-13773-2014, 2014.

676 Slowik, J. G., Stroud, C., Bottenheim, J. W., Brickell, P. C., Chang, R. Y. W., Liggio, J.,  
677 Makar, P. A., Martin, R. V., Moran, M. D., Shantz, N. C., Sjostedt, S. J., van Donkelaar,  
678 A., Vlasenko, A., Wiebe, H. A., Xia, A. G., Zhang, J., Leaitch, W. R., and Abbatt, J. P. D.:  
679 Characterization of a large biogenic secondary organic aerosol event from eastern  
680 Canadian forests, *Atmos. Chem. Phys.*, 10, 2825-2845, 2010.

681 Song, Y., Zhang, Y., Xie, S., Zeng, L., Zheng, M., Salmon, L. G., Shao, M., and Slanina, S.:  
682 Source apportionment of PM<sub>2.5</sub> in Beijing by positive matrix factorization, *Atmos.*  
683 *Environ.*, 40, 1526-1537, DOI: 10.1016/j.atmosenv.2005.10.039, 2006.

684 Sun, J., Zhang, Q., Canagaratna, M. R., Zhang, Y., Ng, N. L., Sun, Y., Jayne, J. T., Zhang, X.,  
685 Zhang, X., and Worsnop, D. R.: Highly time- and size-resolved characterization of  
686 submicron aerosol particles in Beijing using an Aerodyne Aerosol Mass Spectrometer,  
687 *Atmos. Environ.*, 44, 131-140, 2010.

688 Sun, Y., Zhuang, G., Tang, A., Wang, Y., and An, Z.: Chemical Characteristics of PM<sub>2.5</sub> and  
689 PM<sub>10</sub> in Haze-Fog Episodes in Beijing, *Environ. Sci. Technol.*, 40, 3148-3155, 2006.

---

690 Sun, Y., Jiang, Q., Wang, Z., Fu, P., Li, J., Yang, T., and Yin, Y.: Investigation of the Sources  
691 and Evolution Processes of Severe Haze Pollution in Beijing in January 2013, *Journal of*  
692 *Geophysical Research: Atmospheres*, 119, 4380-4398, 10.1002/2014JD021641, 2014.

693 Sun, Y. L., Wang, Z., Dong, H., Yang, T., Li, J., Pan, X., Chen, P., and Jayne, J. T.:  
694 Characterization of summer organic and inorganic aerosols in Beijing, China with an  
695 Aerosol Chemical Speciation Monitor, *Atmos. Environ.*, 51, 250-259,  
696 10.1016/j.atmosenv.2012.01.013, 2012.

697 Sun, Y. L., Wang, Z., Fu, P., Jiang, Q., Yang, T., Li, J., and Ge, X.: The Impact of Relative  
698 Humidity on Aerosol Composition and Evolution Processes during Wintertime in Beijing,  
699 China, *Atmos. Environ.*, 77, 927-934, <http://dx.doi.org/10.1016/j.atmosenv.2013.06.019>,  
700 2013a.

701 Sun, Y. L., Wang, Z. F., Fu, P. Q., Yang, T., Jiang, Q., Dong, H. B., Li, J., and Jia, J. J.:  
702 Aerosol composition, sources and processes during wintertime in Beijing, China, *Atmos.*  
703 *Chem. Phys.*, 13, 4577-4592, 10.5194/acp-13-4577-2013, 2013b.

704 Tian, L., Lucas, D., Fischer, S. L., Lee, S. C., Hammond, S. K., and Koshland, C. P.: Particle  
705 and Gas Emissions from a Simulated Coal-Burning Household Fire Pit, *Environ. Sci.*  
706 *Technol.*, 42, 2503-2508, 10.1021/es0716610, 2008.

707 Tian, Y. Z., Wang, J., Peng, X., Shi, G. L., and Feng, Y. C.: Estimation of the direct and  
708 indirect impacts of fireworks on the physicochemical characteristics of atmospheric  
709 PM10 and PM2.5, *Atmos. Chem. Phys.*, 14, 9469-9479, 10.5194/acp-14-9469-2014,  
710 2014.

711 Ulbrich, I. M., Canagaratna, M. R., Zhang, Q., Worsnop, D. R., and Jimenez, J. L.:  
712 Interpretation of organic components from Positive Matrix Factorization of aerosol mass  
713 spectrometric data, *Atmos. Chem. Phys.*, 9, 2891-2918, 2009.

714 Vecchi, R., Bernardoni, V., Cricchio, D., D'Alessandro, A., Fermo, P., Lucarelli, F., Nava, S.,  
715 Piazzalunga, A., and Valli, G.: The impact of fireworks on airborne particles, *Atmos.*  
716 *Environ.*, 42, 1121-1132, 10.1016/j.atmosenv.2007.10.047, 2008.

717 Wang, Y., Zhuang, G., Sun, Y., and An, Z.: The variation of characteristics and formation  
718 mechanisms of aerosols in dust, haze, and clear days in Beijing, *Atmos. Environ.*, 40,  
719 6579-6591, 2006.

720 Wang, Y., Zhuang, G., Xu, C., and An, Z.: The air pollution caused by the burning of  
721 fireworks during the lantern festival in Beijing, *Atmos. Environ.*, 41, 417-431,  
722 10.1016/j.atmosenv.2006.07.043, 2007.

723 Wang, Y., Yao, L., Wang, L., Liu, Z., Ji, D., Tang, G., Zhang, J., Sun, Y., Hu, B., and Xin, J.:  
724 Mechanism for the formation of the January 2013 heavy haze pollution episode over  
725 central and eastern China, *Sci. China Earth Sci.*, 57, 14-25, 10.1007/s11430-013-4773-4,  
726 2014.

727 Yang, F., Tan, J., Zhao, Q., Du, Z., He, K., Ma, Y., Duan, F., and Chen, G.: Characteristics of  
728 PM2.5 speciation in representative megacities and across China, *Atmos. Chem. Phys.*, 11,  
729 5207-5219, 10.5194/acp-11-5207-2011, 2011.

730 Yang, L., Gao, X., Wang, X., Nie, W., Wang, J., Gao, R., Xu, P., Shou, Y., Zhang, Q., and  
731 Wang, W.: Impacts of firecracker burning on aerosol chemical characteristics and human

---

732 health risk levels during the Chinese New Year Celebration in Jinan, China, *Sci. Total*  
733 *Environ.*, 476–477, 57-64, <http://dx.doi.org/10.1016/j.scitotenv.2013.12.110>, 2014.

734 Yao, X., Chan, C. K., Fang, M., Cadle, S., Chan, T., Mulawa, P., He, K., and Ye, B.: The  
735 water-soluble ionic composition of PM<sub>2.5</sub> in Shanghai and Beijing, China, *Atmos.*  
736 *Environ.*, 36, 4223-4234, Doi: 10.1016/s1352-2310(02)00342-4, 2002.

737 Zhang, H., Wang, S., Hao, J., Wan, L., Jiang, J., Zhang, M., Mestl, H. E. S., Alnes, L. W. H.,  
738 Aunan, K., and Mellouki, A. W.: Chemical and size characterization of particles emitted  
739 from the burning of coal and wood in rural households in Guizhou, China, *Atmos.*  
740 *Environ.*, 51, 94-99, 10.1016/j.atmosenv.2012.01.042, 2012.

741 Zhang, J. K., Sun, Y., Liu, Z. R., Ji, D. S., Hu, B., Liu, Q., and Wang, Y. S.: Characterization  
742 of submicron aerosols during a month of serious pollution in Beijing, 2013, *Atmos. Chem.*  
743 *Phys.*, 14, 2887-2903, 10.5194/acp-14-2887-2014, 2014.

744 Zhang, M., Wang, X., Chen, J., Cheng, T., Wang, T., Yang, X., Gong, Y., Geng, F., and Chen,  
745 C.: Physical characterization of aerosol particles during the Chinese New Year's firework  
746 events, *Atmos. Environ.*, 44, 5191-5198, 10.1016/j.atmosenv.2010.08.048, 2010.

747 Zhang, Q., Jimenez, J., Canagaratna, M., Ulbrich, I., Ng, N., Worsnop, D., and Sun, Y.:  
748 Understanding atmospheric organic aerosols via factor analysis of aerosol mass  
749 spectrometry: a review, *Anal. Bioanal. Chem.*, 401, 3045-3067,  
750 10.1007/s00216-011-5355-y, 2011.

751 Zhang, R., Jing, J., Tao, J., Hsu, S. C., Wang, G., Cao, J., Lee, C. S. L., Zhu, L., Chen, Z.,  
752 Zhao, Y., and Shen, Z.: Chemical characterization and source apportionment of PM<sub>2.5</sub> in  
753 Beijing: seasonal perspective, *Atmos. Chem. Phys.*, 13, 7053-7074,  
754 10.5194/acp-13-7053-2013, 2013.

755 Zhao, S., Yu, Y., Yin, D., Liu, N., and He, J.: Ambient particulate pollution during Chinese  
756 Spring Festival in urban Lanzhou, Northwestern China, *Atmospheric Pollution Research*,  
757 5, 335-343, doi: 10.5094/APR.2014.039, 2014.

758 Zhao, X. J., Zhao, P. S., Xu, J., Meng, W., Pu, W. W., Dong, F., He, D., and Shi, Q. F.:  
759 Analysis of a winter regional haze event and its formation mechanism in the North China  
760 Plain, *Atmos. Chem. Phys.*, 13, 5685-5696, 10.5194/acp-13-5685-2013, 2013.

761 Zheng, M., Salmon, L. G., Schauer, J. J., Zeng, L., Kiang, C. S., Zhang, Y., and Cass, G. R.:  
762 Seasonal trends in PM<sub>2.5</sub> source contributions in Beijing, China, *Atmos. Environ.*, 39,  
763 3967-3976, DOI: 10.1016/j.atmosenv.2005.03.036, 2005.

764 Zhi, G., Chen, Y., Feng, Y., Xiong, S., Li, J., Zhang, G., Sheng, G., and Fu, J.: Emission  
765 characteristics of carbonaceous particles from various residential coal-stoves in China,  
766 *Environ. Sci. Technol.*, 42, 3310-3315, 2008.

767

---

768 **Figure Captions:**

769 **Fig. 1.** Time series of meteorological parameters (a) relative humidity (RH) and  
770 temperature (T); (b) wind direction (WD) and wind speed (WS) at the height of 8m  
771 and 100 m; mass concentrations of (c) PM<sub>2.5</sub> and NR-PM<sub>1</sub> + BC and (d) submicron  
772 aerosol species. The extinction coefficient ( $b_{\text{ext}}$ ) at 630 nm is shown in (c). Three  
773 events, i.e., Lunar New Year (LNY), Lunar Fifth Day (LFD) and Lantern Festival (LF)  
774 with significant influences of fireworks are marked in (c). In addition, the classified  
775 clean periods (CPs) and polluted events (PEs) are marked as shaded light blue and  
776 pink areas, respectively.

777 **Fig. 2.** Time series of PM<sub>1</sub> species (Org, SO<sub>4</sub>, NO<sub>3</sub>, NH<sub>4</sub>, Chl, K, KCl, and BC) and  
778 meteorological variables (wind direction (100 m) and wind speed (8 m)) during three  
779 firework events, i.e., (a) Lunar New Year, (b) Lunar Fifth Day, and (c) Lantern  
780 Festival. The two blue arrow lines represent the starting and ending times of fireworks  
781 events.

782 **Fig. 3.** Correlation of PM<sub>1</sub> vs. PM<sub>2.5</sub> with the data segregated into three fireworks  
783 events (LNY, LFD, and LF) and non-fireworks periods (NFW). The blank circles  
784 represent FW data between 18:00 – 23:30 on 9 February which had large influences  
785 from NFW sources.

786 **Fig. 4.** Average chemical composition of PM<sub>1</sub> and OA from fireworks and  
787 background during three FW events.

788 **Fig. 5.** (a) Average mass spectra (MS) of OA during the firework period of Lunar  
789 New Year (23:30, 9 February – 3:30, 10 February) and the period of background (BG,  
790 4:30 – 11:00, 10 February). (b) Comparison of the difference spectrum from (a), i.e.,  
791  $MS_{\text{FW+BG}} - MS_{\text{BG}}$ , with the average LV-OOA spectrum in Ng et al.(2011a). Note that  
792 five  $m/z$ 's, 37 ( $^{37}\text{Cl}^+$ ), 58 ( $\text{NaCl}^+$ ), 60 ( $\text{Na}^{37}\text{Cl}^+$ ), 74 ( $\text{KCl}^+$ ), and 76 ( $\text{K}^{37}\text{Cl}^+ / ^{41}\text{KCl}^+$ )  
793 marked in the figure were dominantly from fragmentation of inorganic salts during  
794 fireworks.

795 **Fig. 6.** Box plots of (a) mass concentrations and (b) mass fractions of aerosol species  
796 for 9 pollution events marked in Fig. 1. The mean (cross), median (horizontal line),  
797 25<sup>th</sup> and 75<sup>th</sup> percentiles (lower and upper box), and 10<sup>th</sup> and 90<sup>th</sup> percentiles (lower  
798 and upper whiskers) are shown for each box.

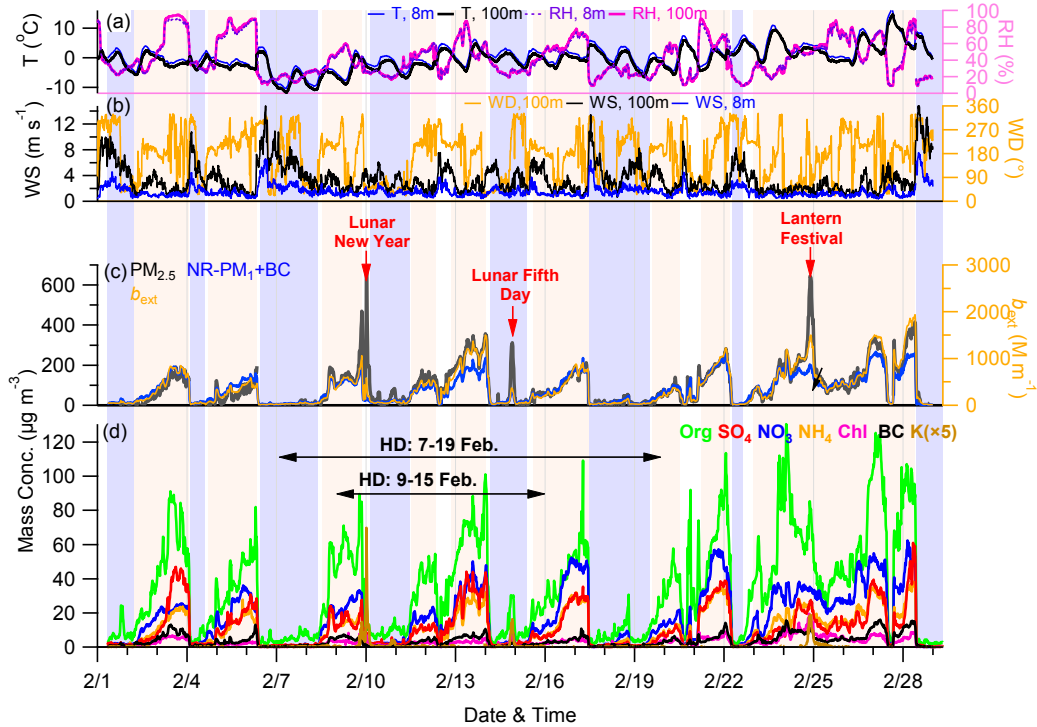
799 **Fig. 7.** Left panel: variations of chemical composition of (a) organics, SNA (=sulfate  
800 + nitrate + ammonium), and others (the rest species in PM<sub>1</sub>); (b) SPM and PPM; and  
801 (c) SOA and POA as a function of PM<sub>1</sub> and organics loadings, respectively. The

---

802 middle and right panels show the diurnal profiles of composition and mass  
803 concentrations, respectively.

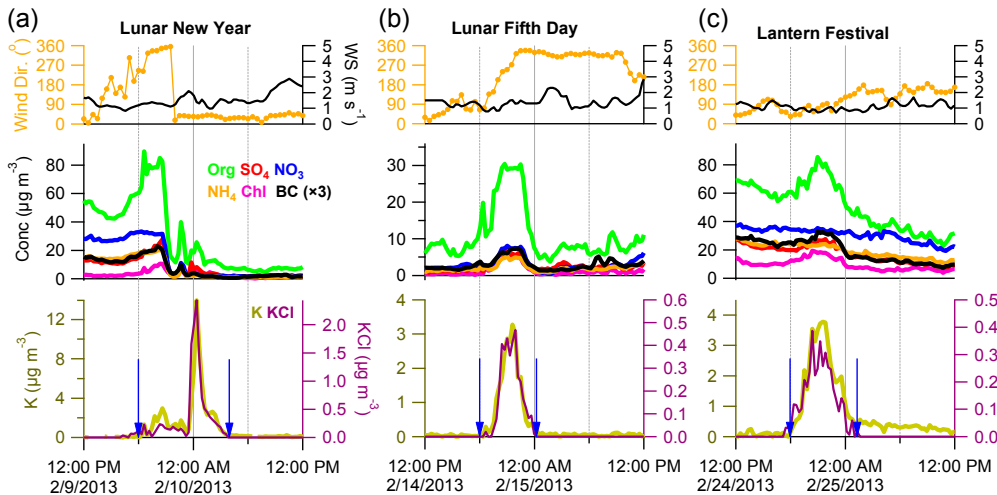
804 **Fig. 8.** (a) Average mass fraction of organics ( $f_{\text{Org}}$ ) as a function of  $\text{PM}_{10}$  mass, and (b)  
805 correlations of extinction coefficients ( $\text{PM}_{2.5}$ ) vs.  $\text{PM}_{10}$  for 9 pollution events (PEs) and  
806 9 clean periods (CPs) marked in Fig. 1. The error bar represents one standard  
807 deviations of the average for each event.

808 **Fig. 9.** The average ratios of aerosol species, gaseous species, PM mass  
809 concentrations, extinction coefficient, and meteorological parameters between holiday  
810 (HD) and non-holiday (NHD) periods. Two different holidays, i.e., the official  
811 holiday of 9 – 15 February and the longer holiday of 7 – 20 February were used for  
812 averages. Also note that the averages were made by excluding clean periods and  
813 firework events during both HD and NHD days. The error bars are the standard errors  
814 of the ratios.



815

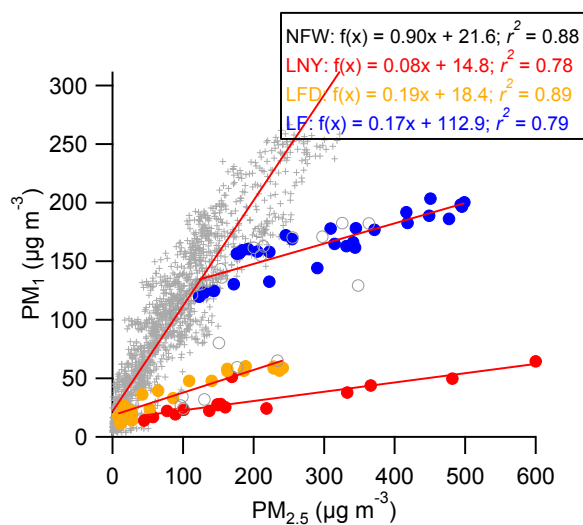
816 **Fig. 1.** Time series of meteorological parameters (a) relative humidity (RH) and  
 817 temperature (T); (b) wind direction (WD) and wind speed (WS) at the height of 8m  
 818 and 100 m; mass concentrations of (c)  $PM_{2.5}$  and  $NR-PM_1 + BC$  and (d) submicron  
 819 aerosol species. The extinction coefficient ( $b_{ext}$ ) at 630 nm is shown in (c). Three  
 820 events, i.e., Lunar New Year (LNY), Lunar Fifth Day (LFD) and Lantern Festival (LF)  
 821 with significant influences of fireworks are marked in (c). In addition, the classified  
 822 clean periods (CPs) and polluted events (PEs) are marked as shaded light blue and  
 823 pink areas, respectively.



824

825 **Fig. 2.** Time series of PM<sub>1</sub> species (Org, SO<sub>4</sub>, NO<sub>3</sub>, NH<sub>4</sub>, Chl, K, KCl, and BC) and  
826 meteorological variables (wind direction (100 m) and wind speed (8 m)) during three  
827 firework events, i.e., (a) Lunar New Year, (b) Lunar Fifth Day, and (c) Lantern  
828 Festival. The two blue arrow lines represent the starting and ending times of fireworks  
829 events.

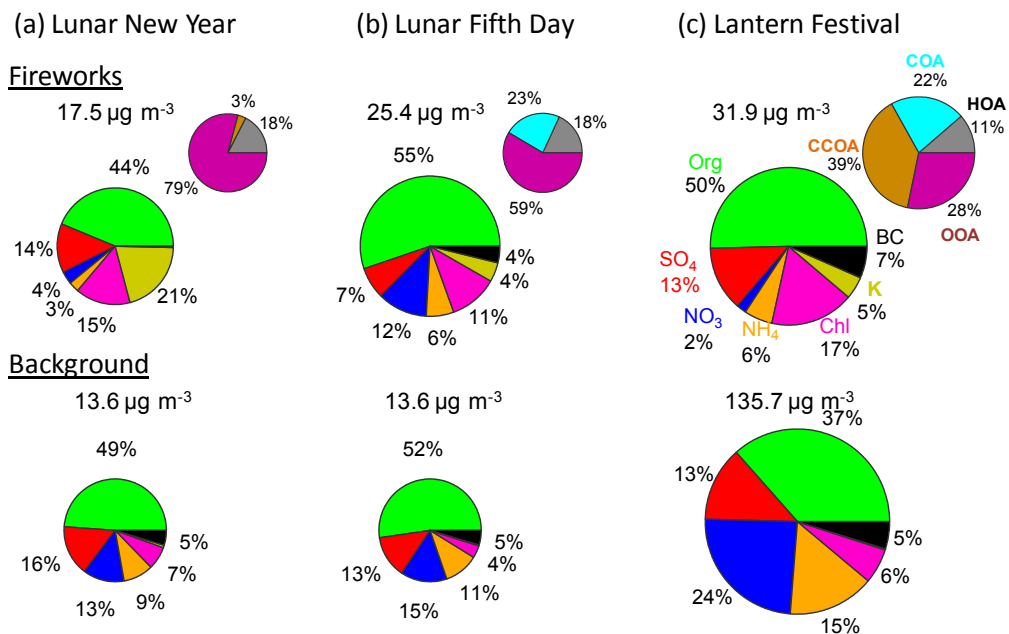
830



831

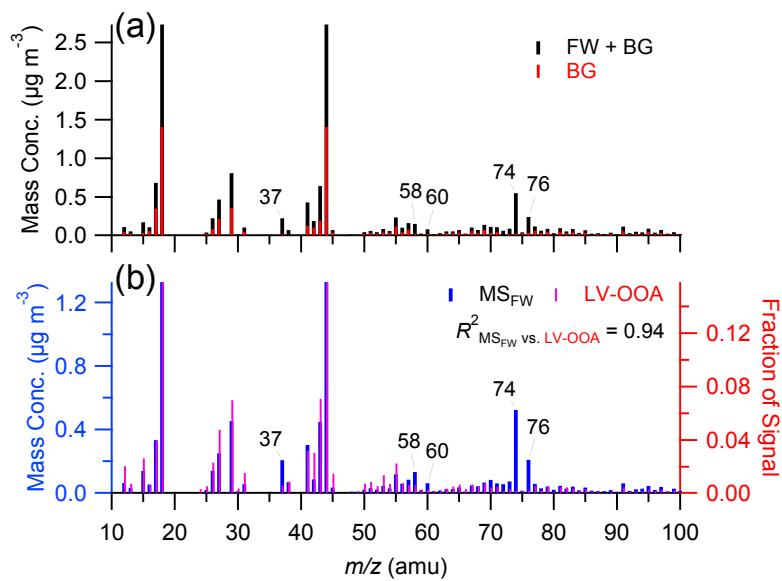
832 **Fig. 3.** Correlation of PM<sub>1</sub> vs. PM<sub>2.5</sub> with the data segregated into three fireworks  
833 events (LNY, LFD, and LF) and non-fireworks periods (NFW). The blank circles  
834 represent FW data between 18:00 – 23:30 on 9 February which had large influences  
835 from NFW sources.





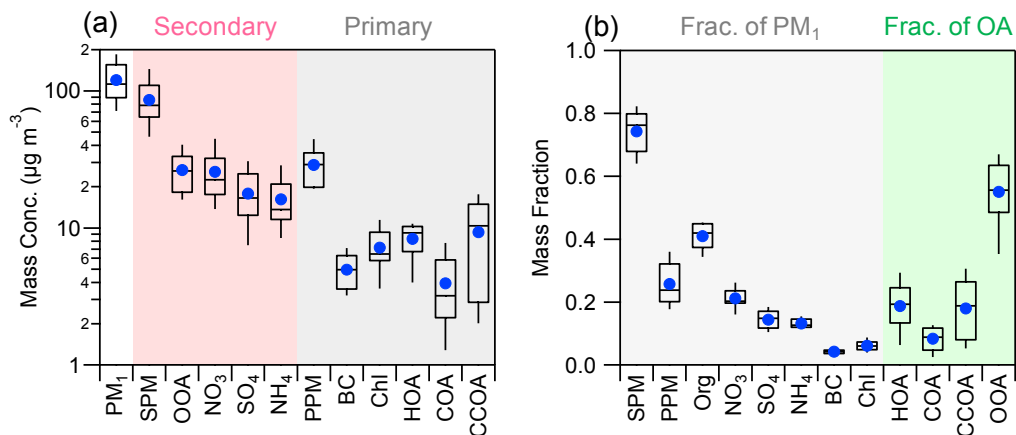
836

837 **Fig. 4.** Average chemical composition of PM<sub>1</sub> and OA from fireworks and  
 838 background during three FW events.



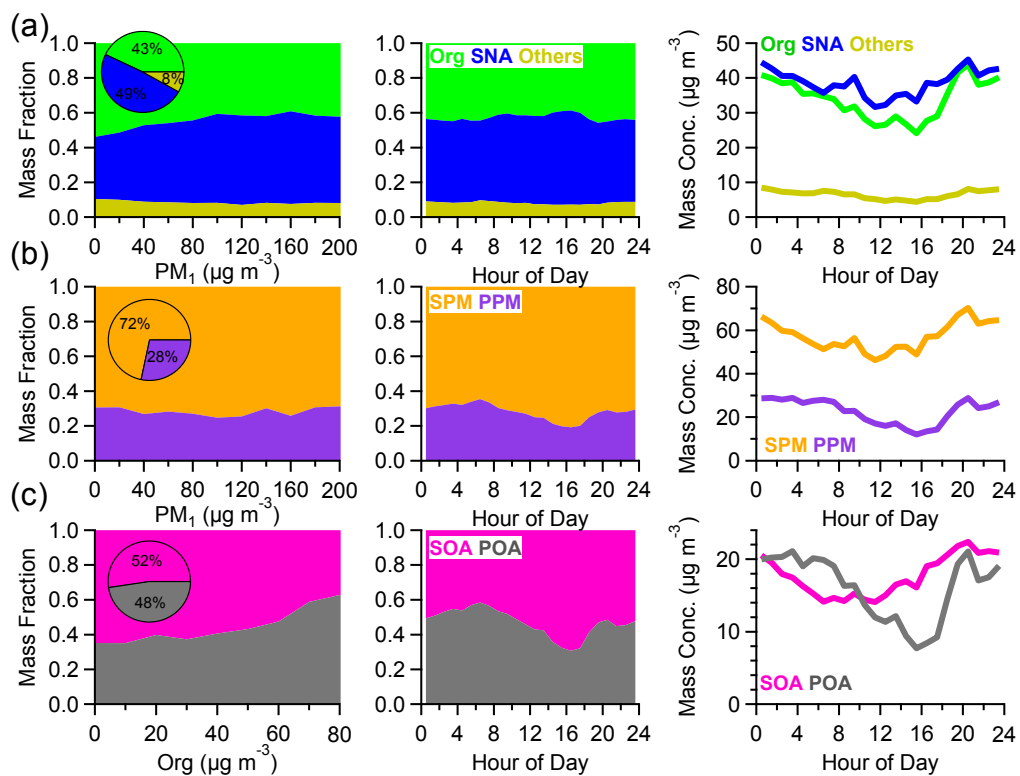
839

840 **Fig. 5.** (a) Average mass spectra (MS) of OA during the firework period of Lunar  
 841 New Year (23:30, 9 February – 3:30, 10 February) and the period of background (BG,  
 842 4:30 – 11:00, 10 February). (b) Comparison of the difference spectrum from (a), i.e.,  
 843  $\text{MS}_{\text{FW+BG}} - \text{MS}_{\text{BG}}$ , with the average LV-OOA spectrum in Ng et al.(2011a). Note that  
 844 five  $m/z$ 's, 37 ( $^{37}\text{Cl}^+$ ), 58 ( $\text{NaCl}^+$ ), 60 ( $\text{Na}^{37}\text{Cl}^+$ ), 74 ( $\text{KCl}^+$ ), and 76 ( $\text{K}^{37}\text{Cl}^+ / ^{41}\text{KCl}^+$ )  
 845 marked in the figure were dominantly from fragmentation of inorganic salts during  
 846 fireworks.



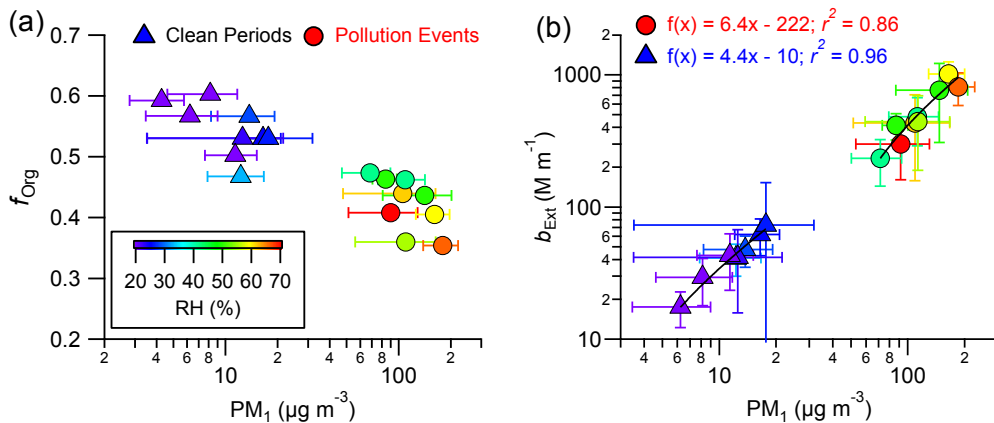
847

848 **Fig. 6.** Box plots of (a) mass concentrations and (b) mass fractions of aerosol species  
 849 for 9 pollution events marked in Fig. 1. The mean (cross), median (horizontal line),  
 850 25<sup>th</sup> and 75<sup>th</sup> percentiles (lower and upper box), and 10<sup>th</sup> and 90<sup>th</sup> percentiles (lower  
 851 and upper whiskers) are shown for each box.



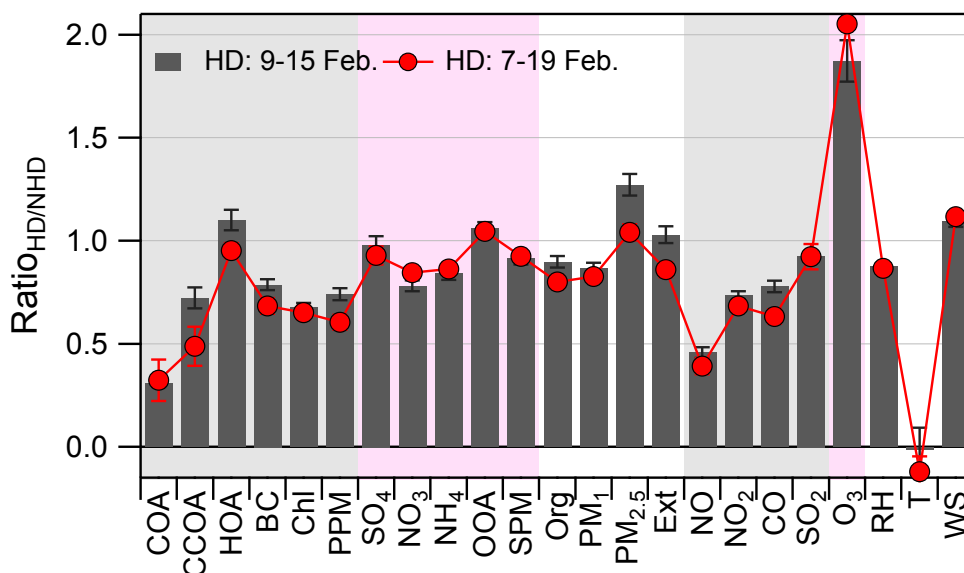
853

854 **Fig. 7.** Left panel: variations of chemical composition of (a) organics, SNA (=sulfate  
 855 + nitrate + ammonium), and others (the rest species in  $PM_1$ ); (b) SPM and PPM; and  
 856 (c) SOA and POA as a function of  $PM_1$  and organics loadings, respectively. The  
 857 middle and right panels show the diurnal profiles of composition and mass  
 858 concentrations, respectively.



859

860 **Fig. 8.** (a) Average mass fraction of organics ( $f_{Org}$ ) as a function of  $PM_1$  mass, and (b)  
 861 correlations of extinction coefficients ( $PM_{2.5}$ ) vs.  $PM_1$  for 9 pollution events (PEs) and  
 862 9 clean periods (CPs) marked in Fig. 1. The error bar represents one standard  
 863 deviations of the average for each event.



864

865 **Fig. 9.** The average ratios of aerosol species, gaseous species, PM mass  
 866 concentrations, extinction coefficient, and meteorological parameters between holiday  
 867 (HD) and non-holiday (NHD) periods. Two different holidays, i.e., the official  
 868 holiday of 9 – 15 February and the longer holiday of 7 – 20 February were used for  
 869 averages. Also note that the averages were made by excluding clean periods and  
 870 firework events during both HD and NHD days. The error bars are the standard errors  
 871 of the ratios.